









## Millions of seafloor pits, not pockmarks, induced by vertebrates in the North Sea

Jens Schneider von Deimling <sup>1✉</sup>, Jasper Hoffmann <sup>2,3</sup>, Jacob Geersen <sup>1,4</sup>, Sven Koschinski<sup>5</sup>, Arne Lohrberg <sup>1</sup>, Anita Gilles <sup>6</sup>, Igor Belkin <sup>7</sup>, Christoph Böttner <sup>1,8</sup>, Svenja Papenmeier<sup>4</sup> & Sebastian Krastel <sup>1</sup>

Seabed pockmarks are among the most prominent morphologic structures in the oceans. They are usually interpreted as surface manifestation of hydrocarbon fluids venting from sediments. Here we suggest an alternative hypothesis of pockmark formation based on latest multibeam echosounder data with a centimeter resolution. In the North Sea, >40,000 enigmatically shaped shallow depressions or ‘pits’ with a mean depth of 0.11 m were documented, that do not resemble known pockmark morphologies. Combining the new echosounder data with information from behavioral biology, physical oceanography, satellite remote sensing and habitat mapping, we conclude that harbor porpoises excavate sediments during benthic foraging. By grubbing the seabed, they cause sandeels to escape from the sediment and initiate the formation of seafloor pits. Time-lapse data reveals that the initially feeding pits serve as nuclei for scouring and eventually merge into larger scour-pits. With the immense number of vertebrates in the ocean, such megafauna-driven macro-bioturbation reshapes the seafloor, modulates sediment transport, and ultimately impacts associated ecosystems on a global scale.

<sup>1</sup>Institute of Geosciences, Kiel University, Otto-Hahn-Platz 1, 24118 Kiel, Germany. <sup>2</sup>Alfred-Wegener-Institute, Helmholtz Centre for Polar and Marine Research, Hafenstraße 43, 25992 List, Germany. <sup>3</sup>Marine Geology and Seafloor Surveying, University of Malta, 37, Triq ta' Xmiexi, 1752 Msida, Malta. <sup>4</sup>Leibniz Institute for Baltic Sea Research Warnemünde, Seestraße 15, 18119 Rostock, Germany. <sup>5</sup>Meereszoologie, Kühlwandweg 12, 24326 Nehnten, Germany. <sup>6</sup>Institute for Terrestrial and Aquatic Wildlife Research at University of Veterinary Medicine Hannover, Foundation, Werftstraße 6, 25761 Büsum, Germany. <sup>7</sup>College of Marine Science and Technology, Zhejiang Ocean University, Zhoushan, China. <sup>8</sup>Department of Geoscience, Aarhus University, 8000 Aarhus, Denmark. ✉email: [jens.schneider@ifg.uni-kiel.de](mailto:jens.schneider@ifg.uni-kiel.de)

In the medical realm, pockmarks are well known as deep scars on the skin and are obviously of biogenic nature. In geoscience, pockmarks are referred to as cone-shaped depressions in the seabed<sup>1</sup>. Geologic pockmarks are traditionally believed to result from fluid (i.e., gas or liquid) venting with erosive agents emerging from beneath the seabed<sup>1</sup>. They were first observed in the 1970s within clastic sediments offshore Nova Scotia, Canada<sup>2</sup>. Now, about five decades after their initial discovery, it has become clear that pockmarks are among the most widespread morphologic features in the oceans<sup>1</sup>. Individual pockmarks, as well as large pockmark fields, containing hundreds to many thousands of features, have been reported from around the globe across a range of marine and lacustrine provinces. These include deep ocean basins, fjords, marginal seas, estuaries, continental shelves, and slopes, as well as lakes<sup>3–9</sup>. When fluids vent into the water they suspend the surrounding sediments and nutrients, which are then transported away by bottom currents. This leaves behind characteristic pockmark depressions varying in diameter from less than 1 m to more than several hundreds of meters. Their depth is roughly correlated to their diameter and ranges from centimeters to tens and hundreds of meters for giant pockmarks discovered by echosounding techniques<sup>1,7,10,11</sup>. The main fluid venting component emitted from pockmarks appears to be methane (natural gas) while closer to the coasts pockmarks are also associated with groundwater discharge<sup>3</sup>. In some cases, fluid venting appears unlikely from a geological perspective and no indications for fluid venting were identified<sup>12,13</sup>. In recent years, non-fluid-related mechanisms have been proposed as formation mechanism for pockmarks or similarly shaped seafloor depressions in general (e.g., pockforms<sup>14</sup>). These include erosion and scouring around natural or anthropogenic obstacles at the seafloor<sup>12,15,16</sup>, benthic feeding activity of gray whales<sup>17,18</sup>, and bottom grubbing by fish, though, the topic is discussed controversially<sup>19–22</sup>.

A marine region littered with seafloor depressions is the North Sea, one of the most prolific sedimentary basins in respect to hydrocarbon exploration<sup>1,23,24</sup>. It is known for its thousands of oval or round shaped pockmarks along the North Sea Graben with sizes ranging from a few centimeters to sometimes >100 m, that are so far mainly interpreted to result from fluid seepage<sup>1</sup>. In the German Bight of the North Sea, a recent study revealed an abruptly emerging pockmark field north of Heligoland (Fig. 1) with more than 15,000 depressions with diameters in the tens of meter-scale and a maximum depth of around 0.2 m<sup>25</sup>. Remarkably, the Heligoland pockmarks were found to emerge and disappear within a couple of months, which was attributed to episodic methane degassing events and storm sediment infilling<sup>25</sup>. The methane discharge of such an event was estimated to about 5 kt<sup>25</sup>, which appears unlikely in the light of our high-resolution database and analysis.

Here, we present a new interpretation for the formation of seafloor depressions in the German Bight and predict that the underlying mechanisms apply globally but have been overlooked so far. Broadband multibeam echosounder data with centimeter resolution reveal morphological characteristics that challenge a methane-related geological formation of the pockmarks. Combining our hydroacoustic data with information from behavioral biology, physical oceanography, satellite remote sensing, and habitat mapping, we explore the link between biological forcing and geological pattern and formulate hypotheses on the formation mechanism of the seafloor depressions. Using a hitherto unknown foraging behavior, the most abundant small cetacean species in the North Sea, the harbor porpoise (*Phocoena phocoena*), excavate the depressions in the sandy seafloor while foraging between 20 and 35 m water depth (Fig. 1). We therefore refrain from the word ‘pockmark’ and instead use the expressions ‘pits’ (<10 m diameter) and ‘pit-scours’ (≥10 m diameter) to

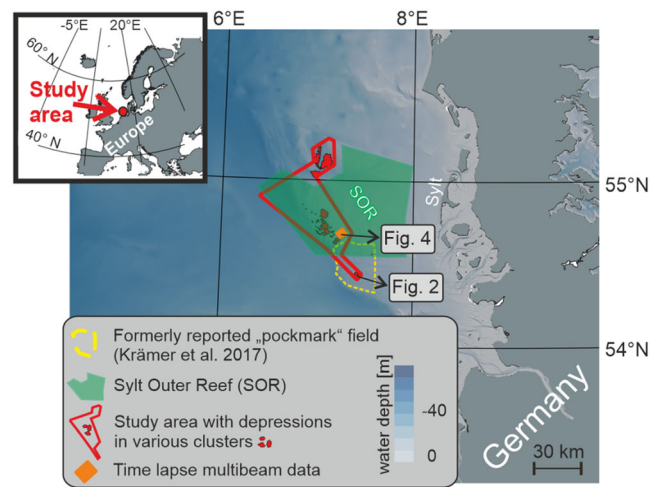


**Fig. 1 Overview map of the study area in the German Bight of the North Sea.** The red and yellow-dashed polygons outline regions with seafloor depressions. In the yellow area termed ‘pockmark’ field, more than 15,000 depressions had been reported<sup>25</sup>. We confirmed the existence of the depressions in this area. Farther North (red polygon, our study area), we found an even larger quantity of 42,458 depressions in various clusters with exceptionally shallow incisions with 0.11 m mean depth (Figs. 2, 3). Here, repeat surveys allow a time-lapse view of the depressions (Fig. 4). The overview bathymetry of this chart is based on the latest EMOdnet 2020 data release. All cruise track plots are given in Supplementary Fig. 1.

describe the depressions. Considering the immense number of megafauna in the ocean hunting for benthic prey, such macrobioturbation has a huge potential in reshaping the seafloor, modulating sediment transport and nutrient supply, and ultimately impacting associated ecosystems on a global scale. Our findings have wide implications for geological facies definition and behavioral biology, and the gained knowledge can help to improve marine environmental protection in the North Sea.

Our work was conducted in the German Bight in the southeastern part of the North Sea (Fig. 1). The study area is located within the Sylt Outer Reef (SOR) which is characterized by a postglacial sedimentation setting on a shallow shelf with mostly less than 40 m water depth. Fine-grained tills deposited by grounded ice are covered by tens-of-meters-thick fluvial sand and gravel layers, as well as interglacial clay and silt deposits<sup>26</sup>. The shallow SOR sediments consist of <10 m of reworked sands of Early Holocene, Pleistocene and Neogene age overlying the morainal deposits which are occasionally exposed, revealing boulders and rocky reef systems<sup>27</sup>. The research area is in water depth ranging between 20 and 40 m and hosts fine to medium-grained sands with a low (<5%) mud content<sup>28</sup>. In some places coarse-grained sands occur, occasionally forming so-called sorted bedforms<sup>29,30</sup>. The German Bight is an area characterized by strong tidal currents of almost 1 m/s<sup>31</sup> and mesoscale variability in physical properties with tidal mixing fronts parallel to the coast<sup>32</sup>.

## Results

**Modern echosounding of seafloor depressions in the German Bight.** We re-surveyed the deeper parts of the SOR area north of Heligoland using modern broadband multibeam echosounder systems (MBES) with centimeter range resolution (Fig. 1). At the first glimpse on the interpolated bathymetric chart (Fig. 2a) the depressions resemble the typical appearance of pockmarks. They are located in water depth of 28–28.5 m, surrounded with a flat and otherwise featureless seabed (Fig. 2).

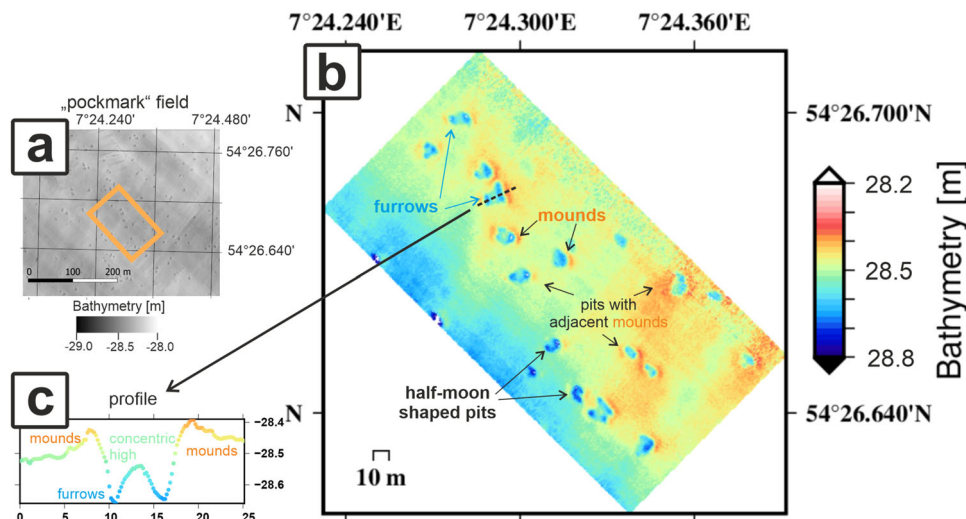


**Fig. 2** High-resolution bathymetric data from the formerly reported pockmark field north of Heligoland. **a** Multibeam echosounder data visualized in an interpolated and equidistant space digital terrain model manner spanning a 500 by 500 m wide area. The 1 by 1 m lateral resolution data reveal approximately one dozen of circular depressions in each tile (0.02 km<sup>2</sup>). **b** Color-coded bathymetric soundings in a point cloud close-up, no interpolation applied (400 kHz). The horizontal resolution is 0.2 m and the vertical acoustic range resolution-0.01 m. Owing to the centimeter-scale resolution, enigmatic shapes emerged that do not resemble classic pockmark morphologies. **c** Depth profile across a characteristic depression, resolving two 0.1 m deep furrows separated by a 0.05 m high in the middle, and surrounded by 0.05 m high mounds. Such ultra-high vertical resolutions become only feasible at short sonar ranges with modern broadband multibeam echosounders coupled with sophisticated inertial measurement units as applied during our surveys.

However, instead of looking exclusively at interpolated digital terrain models (Fig. 2a), we also inspected the very clean MBES soundings in close-up views in a point cloud manner (Fig. 2b). At this centimeter vertical accuracy, that is feasible with a modern near-range broadband MBES and a coupled inertial navigation system, it becomes clear that most depressions (hereafter referred to as pits) are not circular, but they appear with peculiar shapes and morphologies (Fig. 2b). We document furrows, concentric highs within the pit, and mounds on their rims (Fig. 2c) a few centimeters higher than the surrounding seabed. Some pits have a half-moon shape (Fig. 2b). Sometimes the mounds appear on one, sometimes on two sides of the pit, sometimes all around the pit, or half-moon or crescent dune like, yet we were unable to identify a preferred orientation of the features. The spatial alignment of the individual pits varies, e.g., linear, curvilinear, radial, or clustered. When aligned, we often observe equidistant spacing between individual pits in alignments extending from a few meters to tens of meters (Fig. 2b). The average depth of single pits ranges around 0.1 m and hardly exceeds 0.2 m.

To evaluate whether the unconventional pits represent a local particularity or if they occur throughout the area, we followed the tidal mixing front (Supplementary Fig. 2) and covered large parts of the SOR. In the area outlined by the red polygon (Fig. 1), we re-examined 4965 km of existing MBES profiles covering a total area of 2128 km<sup>2</sup>, collected time-lapse bathymetric data (orange box, Fig. 1), and analyzed sidescan and sub-bottom profiler records (Supplementary Fig. 3, 4). In the new survey region, our automatic mapping algorithm detected 42,456 pits (Supplementary Fig. 3) covering about 9% of the seafloor in that area. The pits resemble a truncated cone and show a remarkably small average pit depth of only 0.11 m. For the vast majority of the pits, the depth varies from 0.05 to 0.2 m, with a mode of 0.08 m and a Gaussian-shaped distribution (Fig. 3). Pit depths barely vary with the size of the pit (Fig. 3). The mean surface area of a pit is 297 m<sup>2</sup> which translates into a circular-equivalent radius of 9.7 m. Virtually no pits were found with depths larger than 0.2 m, even when they span 50 m in diameter.

Alongside the MBES data we also recorded towed sidescan data that showed to be unreliable for the detection of pits (Supplementary Fig. 3). The thickness of Holocene sediments on top of the Pleistocene varies roughly between 0 and 10 m (Supplementary Fig. 4). We found no correlation between the occurrence of pits and Holocene sand sediment thickness, nor any acoustic blanking, bright spots, or flares being reliable acoustic proxies for shallow gas or gas ebullition.

**Time-lapse evolution of seafloor pits in the German Bight.** To explore the temporal evolution of the seafloor pits we conducted repeat MBES surveys covering the same area in May 2021 and November 2021 (Fig. 4). Both datasets were acquired with the same MBES, during similar survey conditions. The acoustic records revealed numerous pits with diameters between 10 and 20 m in the fine to medium-grained sand. They host the characteristic irregular, non-circular shapes, adjacent mounds, and overall shallow incision depth of 0.1–0.2 m relative to the surrounding flat sandy seafloor. Close inspection of the time-lapse data reveals that the pits in the November data appear smoothed-out compared to the May dataset, with local enlargements after the six months period. Some of the pits seem to commingle producing an irregular and uneven seafloor morphology. In particular, individual pits have widened and single pits have merged, thereby contributing to the above-mentioned irregular features and uneven seafloor morphology. But even more importantly, numerous smaller pits that must have evolved during the six months' time period appeared. Those new pits are ~0.2 m deep and only 2–6 m wide. Most of the new pits are slightly elongated without any noticeable preferred orientation. They occur predominantly in areas where pits have been observed previously but rarely also in some areas that didn't show any sign of pits in May 2021.

## Discussion

For the Central North Sea, widespread evidence of fluid seepage (mainly hydrocarbon) from hydroacoustic and geochemical

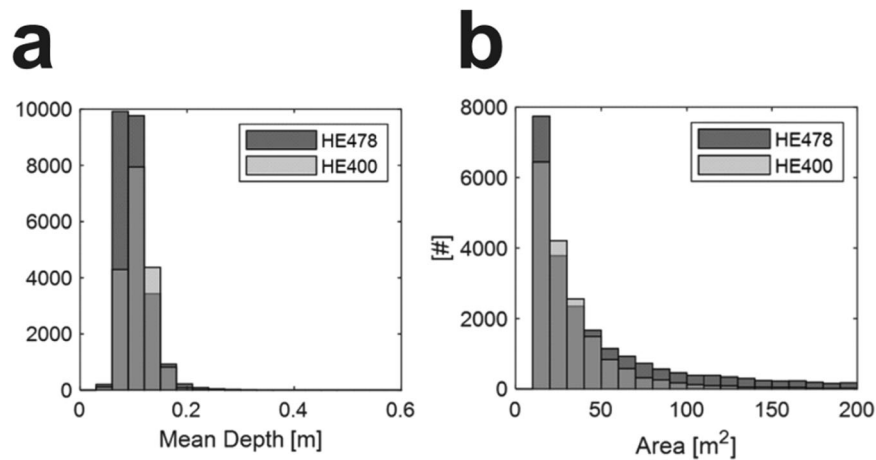


**Fig. 3** Histogram analyses of seafloor pits and pit-scours mean depth and area. **a** Gaussian-like mean depth of pits and pit-scours. **b** Skewed area distribution of pits and pit-scours. For the statistical analyses, data acquired during research cruises HE400 and HE478 were used, comprising 98.2% of all analyzed areas in this study (Supplementary Table 1).

data exists<sup>1</sup>. Only limited data, however, suggests active fluid seepage from the seafloor in the German Bight. Here, fluid seepage was only documented from the Dogger Bank and the Palaeo-Elbe River in the northwestern part of the German Bight<sup>33</sup> or related to drilling and hydrocarbon exploration<sup>34</sup>. As the seafloor in the German Bight was intensively studied over the past decades (for example, >40,000 seabed samples were taken between the 1960s and 2010<sup>28</sup>) the widespread absence of fluid seepage seems to be a real geologic phenomenon. The shallow sedimentary strata in our research area consists of a thin drape (<10 m) of clastic Holocene sediments of fine to medium and gravelly sands with occasional boulders which are underlain by Pleistocene sediments (Supplementary Fig. 4). Holocene sediments are depleted in organic matter which is mainly exported from the shelf into the Norwegian Skagerrak Channel<sup>35</sup>. Figure 4 demonstrates the high mobility of the upper fine to medium-grained sands which seem to be remobilized on a regular basis, as also reported in other studies conducted nearby<sup>15</sup>. The mobile, fine to medium-grained but permeable sands with low organic matter content andoxic bottom water conditions seem unlikely to store or form large amounts of methane gases, which may explain the overall absence of documented seepage sites in the area.

Neither from previous studies, nor from our 4965 km of acoustic sub-bottom profiling, which is very sensitive to shallow gas, we find evidence for acoustic blanking or other indications for free gas. The previously reported ‘gas flare’<sup>25</sup> is the only one despite the tens of thousands of depressions, it is only 1.8 m high, and its sonar pattern is ambiguous. It does not meet flare imaging criteria for unambiguous gas bubble detections<sup>10,36</sup>. Given the high abundance of fish in the area, we propose a fish school as the more likely explanation for the observed echo anomaly. The only location near Heligoland with some acoustic blanking appears southeast of the island, in deeper areas outside of the SOR<sup>37</sup>. A previous study<sup>25</sup> documented depressions exclusively in regions where the thickness of the Holocene sands is below 1 m. However, based on our MBES and sub-bottom profiling data we document pits also farther north with 5 m and more of Holocene sands covering the Pleistocene (Supplementary Fig. 4). No indications of gas migration pathways (e.g., pipes or chimneys) are observed. The German Bight was intensely investigated by researchers and fisheries over the past decades. But neither fisheries reports, nor underwater video camera footage of the pits provided any indications for methane-related chemosynthetic communities or methane-derived authigenic carbonates<sup>1</sup>. Several

studies reported dissolved methane concentrations near Heligoland around 4 nM, which is close to the background concentration in the rest of the North Sea around 3.5 nM. Elevated methane concentrations towards the Elbe river mouth are caused by riverine discharge<sup>38,39</sup>.

The above considerations argue against methane seepage as trigger for the formation of the tens of thousands of depressions in the German Bight which were previously referred to as pockmarks<sup>25</sup>. In the following we argue that harbor porpoises, small, toothed cetaceans with an estimated abundance of 23,219 (95% CI: 16,621–34,104)<sup>40</sup> individuals in the German Bight, cause the pits on the seafloor while foraging on benthic fish. The initially small feeding pits (Fig. 4) serve as nuclei for subsequent scouring. Under strong tidal flow of up to 1 m/s<sup>31</sup> bottom currents scour and re-shape the pits before they ultimately disappear during episodic storms (Fig. 5).

Harbor porpoises are capture suction feeders<sup>41</sup> that prefer benthic fish as their diet<sup>42</sup>, but the exact mechanism of their benthic forage has not yet been observed in the wild. It is known that they perform U-shaped dives with considerable time spent foraging at the bottom<sup>43</sup>. In several cases, sand particles were found in the stomachs of stranded animals<sup>44</sup>. The bottom grubbing foraging begins when the animals position their bodies vertically in the water in search of benthic prey, as has been documented for harbor porpoises in captivity<sup>45</sup>. They point their heads downward, echolocating towards the sediment. Subsequently, the prey is attacked by digging approximately 0.1–0.2 m deep into the sediment with their snout<sup>45–47</sup>, thus excavating sediment and creating furrows with adjacent mounds. This technique allows the animals to efficiently feed on benthic fish. Cetaceans acting as eroding agents on the seafloor have formerly been suggested<sup>17,18</sup>, but direct evidence for such benthic feeding is difficult to obtain, and very little follow-up research about megafauna erosion was published.

Oval pits of similar dimensions compared to the pits north of Heligoland were found in the Bering Sea<sup>17</sup>. Here, in a similar postglacial setting consisting of fine sands, they have been interpreted to be caused by gray whales (*Eschrichtius robustus*) feeding on benthic shrimp by suction feeding<sup>17</sup>. Associated sediment plumes in the water column document their seabed erosion potential during and after benthic feeding activity<sup>48</sup>. Aligned pits, similar to those presented in this study but in deeper waters, were interpreted to be caused by large bathypelagic vertebrates<sup>49,50</sup>. Pioneering studies also showed that small furrows from benthic feeding of walrus (*Odobenus rosmarus*)

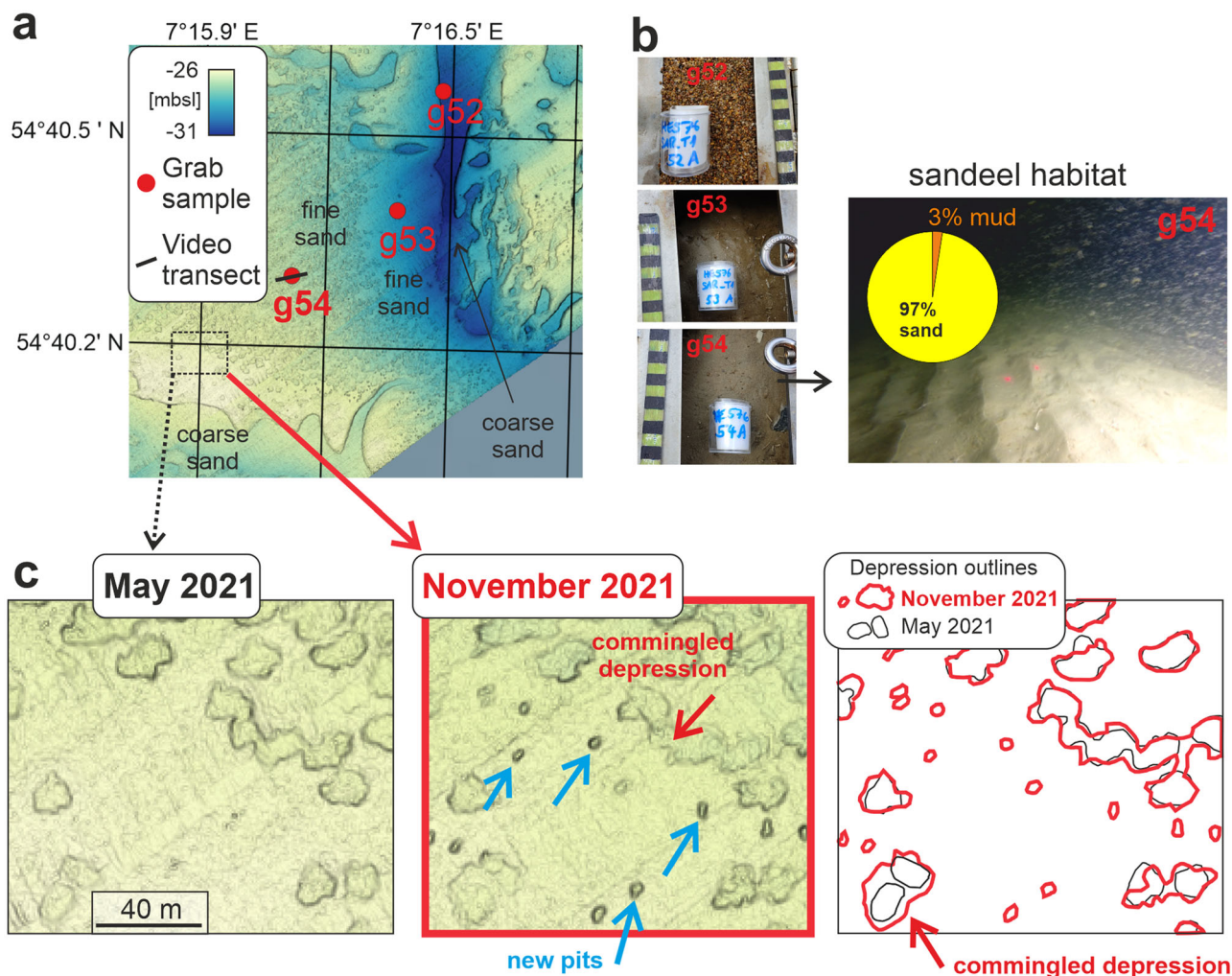


**Fig. 4** Time-lapse bathymetric data across some seafloor pits highlighting morphologic differences between May and November 2021 (see Fig. 1 for location). **a** Overview plot from May 2021. The MBES data reveals pits with less than 10 m diameter and over 60 m diameter commingled depressions within the fine to medium sand. No pits were identified in the coarser sand in the deeper areas. **b** three grab samples were analyzed (g52–g54) and a video transect was sailed across the pits on the grab sample site g54. While the samples g53 and g54 taken in the pits area consist of the same fine to medium-grained sand (g53: 17% medium sand, 69% fine sand, 10% very fine sand, 3% silt, 1% clay and g54: 24% medium sand, 66% fine sand, 7% very fine sand, 3% mud), g52 consists of coarse sands with fine gravels (g52, 65% fine gravel, 32% coarse sand, <3% medium to very fine sand and mud). A still picture of the seafloor at g54 shows a featureless sandy seafloor with sand ripples (laser points plot in 0.1 m distance), pits remained invisible in the optical video records. **c** MBES time-lapse data revealing ‘new’ pits with diameters of 2–6 m emerging in the November dataset compared to the May dataset.

can be detected with high-frequency near-range sonar data<sup>18</sup>. The remarkably consistent shallow mean depth of the pits (Fig. 3) is also in line with studies reporting on fish as eroding agent coming from above, forming decimeter-scale seafloor pits.

Dolphins are known to spend a substantial amount of time with bottom grubbing feeding behavior<sup>51</sup>. Visual underwater images provided direct evidence of macro-benthic bioturbation by dolphins<sup>51</sup>. Recently, more sophisticated and cooperative foraging strategies have been reported for bottlenose dolphins (*Tursiops truncatus*), which conducted mud-ring feed by using their tails to erode the seabed<sup>52</sup>. Harbor porpoises are physiologically and intellectually able to perform similar cooperative feeding strategies thus possibly creating the enigmatic pattern we show (Fig. 2).

Prey availability at sea is largely determined by the oceanographic setting and nutrient supply. Increased aggregation of phytoplankton, zooplankton, and small fish occurs at tidal mixing fronts<sup>53</sup>. The North Sea is characterized by high primary productivity and identified as one of the Large Marine Ecosystems in

the World Oceans<sup>54</sup>. Productivity is especially high along the tidal mixing front, which trends parallel to the coast across the SOR<sup>32,55</sup> (Supplementary Fig. 2). Porpoise abundance was reported particularly high during spring in our research area<sup>56</sup>, which is likely linked to the presence of the tidal mixing front (Supplementary Fig. 2). This is in line with observations for preferred foraging of harbor porpoise in the vicinity of tidal jets<sup>57</sup>. Resolving the location of the tidal mixing front at the time of our sonar mapping through satellite sea surface data (Supplementary Fig. 2) shows that it coincides with the area of the most pristine pits (Fig. 2).

Along the tidal mixing front, sandeels (*Ammodytes marinus*) are known to occur in large quantities in the North Sea<sup>58</sup> (Fig. 6). Sandeels feed on zooplankton during summer daytimes, but most of the time they hide and even hibernate up to 0.4 m deep buried in fine to medium sandy seafloor for shelter and energy savings reasons<sup>59</sup>. Thereby sandeels challenge predators to grub into the sediment. Sandeels are one of the preferred preys for North Sea harbor porpoises and account for 18–20% of their diet<sup>42,44</sup>. Each

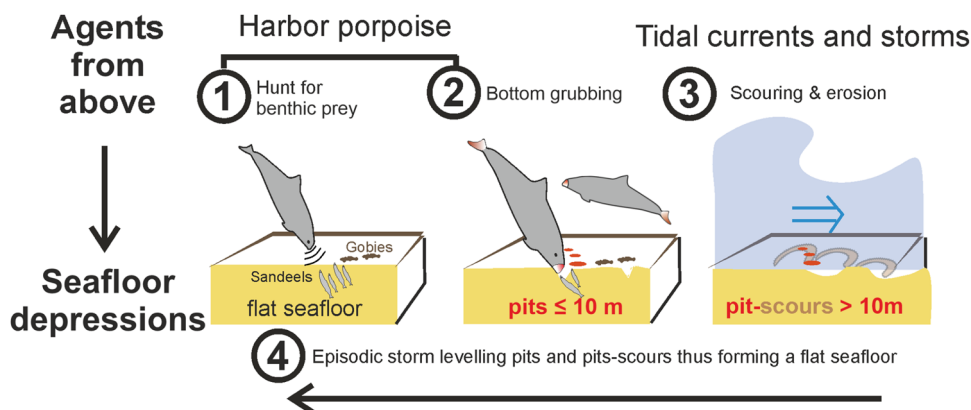


**Fig. 5 The harbor porpoise pits model.** Schematic sketch of seafloor pits and pit-scours evolution through biological and oceanographic eroding agents both coming from above the seabed. We suggest the following model for the formation of the pits and pit-scours. Phase 1: Harbor porpoise acoustically search for buried fish (sandeel) using their sonar on a flat seafloor. Phase 2: Bottom grubbing similar to the one observed for dolphins and gray whales, resulting in decimeter to meter large pits with a distinct morphology. Phase 3: The pits act as nucleation points for bottom currents to initiate scouring and formation of pit-scours, erosion and sediment transport, which subsequently leads to the commingling of individual pit-scours, resulting in larger structures on the seafloor (Fig. 4). Phase 4: Episodic but severe storms predominantly in winter completely level out the structures over time and eventually form a flat seafloor, setting the start point for phase 1, thus closing the evolution cycle.

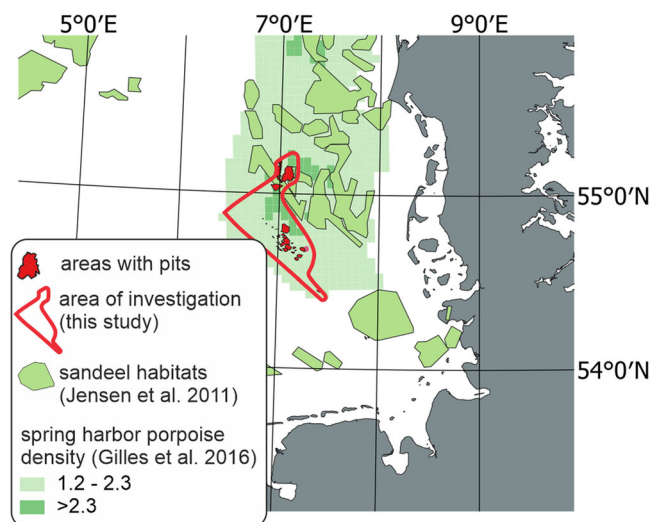


**Fig. 6 Map indicating spatial correlation between seafloor pits, sandeel habitats, and harbor porpoise density model prediction.** The area covered by pits and pit-scours comprises 8.7% of the investigated area. All pits appear between 20 and 35 m water depth within a radius of 10 nm (18.5 km) of areas inhabiting sandeels<sup>58</sup>, one of the preferred preys in harbor porpoise diets. In addition, the pits appear in or close to the areas predicted as maximum likelihood for harbor porpoises in spring<sup>56</sup>, the period where the majority of our data were acquired.

of the 42,456 pits documented in this study is located within known sandeel habitats<sup>58</sup> (Fig. 6). We consulted a probability density harbor porpoise model<sup>56</sup>, which includes proximity to tidal mixing front and sandeel habitats, to find that the highest harbor porpoise abundance in spring appear in the vicinity of our seafloor pits (Fig. 6).

By grubbing the seabed, porpoises may flush out nearby sandeels from the sediment. As sandeels are schooling fish, the expulsion of individuals may result in the entire school attempting to escape predation in an eroding manner. Similar fish like the Pacific sand lance (*Ammodytes personatus*), are known to be an important component of the diet of seabirds, harbor seals, and other fish such as salmon<sup>60</sup>. The latter have been observed to carry scars on their heads, indicating that they have scraped the

seabed (pers. comm. H. Gary Greene). For the North Sea, other large vertebrates such as seals are known to dive to the seabed feeding on benthic fish, and should therefore be considered in future research on macrofauna benthic bioturbation.

Harbor porpoises, representing small endothermic predators in temperate waters, have high energy requirements and need to forage permanently<sup>61</sup>. They feed on small fish (<0.3 m) such as herring, cod, flatfish, sandeel, and gobies<sup>42,44</sup>. The weight fractions of benthic species in their diets include 21% sandeels, 26% gobies and 11% flatfish in the German North Sea<sup>44</sup>. From this, we estimate the share of benthic fish consumed by all harbor porpoises predicted to occur in the study area (Fig. 6), which are 4078 individuals (95%CI: 2893–5107) in spring. On average a single harbor porpoise consumes 1.96 kg/day<sup>43</sup>, the ‘benthic fraction’ of this diet accounts to 1.14 kg/day. The mean fraction of sandeel alone constitutes 413 g or 31 individual fish per day, assuming an average weight of 13 g per fish (own data). This adds up to over 125,743 sandeels assumed to be consumed per day in the area of the observed pits. This simplified calculation demonstrates that from their size and known behavior, the population of harbor porpoise in the North Sea is capable of producing millions of feeding pits through macro-bioturbation each year.

It is difficult to imagine that individual eroding grubs into the sediment produce pits up to 50 m diameter. The German Bight is characterized by strong tidal currents, severe storms predominantly during winter, and high waves. The formerly mentioned ‘pockmark’ field was found to wax and wane over weeks to months<sup>25</sup>. We attribute the levelling of the pits to severe storms when the wave-induced orbital motion reaches down to the seafloor in 25 m depth. Scouring by tidal bottom currents likely acts as the second eroding agent on the seabed modulating the pits over time (Figs. 4, 5). Pockmarks can occur as self-scouring features and can be modified by bottom currents after their initial formation<sup>62</sup>. A depression in the seafloor introduces turbulence of the bottom current which in turn further removes the sediments. Since the tides in the German Bight introduce a rotating rather than bi-directional current regime<sup>63</sup> we would assume that initial depressions are not elongated in one direction but rather non-directional. In this setting, the smaller pits (<10 m diameter) likely act as nuclei for the subsequent formation of pit-scours (≥10 m). This includes commingling of individual pits to form larger pit-scours (Fig. 4).

Sorted bedforms and specifically rippled scour depressions (RSD) are common features in many tidal nearshore environments. They are associated with the co-existence of different sediment grain sizes<sup>64,65</sup>, where the depressions are composed of coarser grained material. RSDs are widely distributed on the SOR and also observed in our datasets in regions where gravelly coarse sands are present in the bathymetrically deeper parts (Fig. 4). However, pits occur exclusively within fine to medium sandy seafloor, and not in the gravelly coarse sands (Fig. 4, grab sample g53 and g54).

The exact mechanisms of initial pit formation and subsequent scouring remain unobserved. We interpret the most distinct seafloor pits presented in Fig. 2 and Fig. 4 to represent relatively pristine feeding pits that have the potential to act as nuclei for subsequent current scouring. The larger ones are partly formed by merging of smaller individual pits through scouring and erosion.

With the harbor porpoise pits hypothesis for the German Bight, we stimulate a discussion on seabed shaping mechanisms and show a possibility to identify feeding grounds for marine vertebrates based on hydroacoustic data. Particularly in large marine ecosystems with high primary production<sup>54</sup>, macro-bioturbation by benthic megafauna plays a major role in reshaping the seafloor. Such macro-bioturbation and its erosional impact have largely been overlooked since the first reports on pockmarks in the 1970s. Based on high-resolution multibeam data, we provide a new explanation of the origin of tens of thousands of pits on the seafloor in the German Bight and suggest that, contrary to previous speculations, the greenhouse gas methane is not involved in their formation. Millions of similar seafloor pits likely exist temporally in the North Sea and elsewhere around the Globe. These, however, usually remained undetected given limited spatial and temporal resolution in legacy echosounder data.

The possibility to identify feeding grounds on the seafloor with latest sonar technology provides huge potential for environmental protection, sustainable fisheries, and better understanding of ecosystem services. Continental shelves and marginal seas are currently considered for massive offshore wind farming and related seabed infrastructure thus threatening benthic habitats. Our study outlines that feeding grounds can be mapped out with modern near-range sonars. With such new knowledge the existing marine environmental protection strategies can be refined, and economical-ecological conflicts can be mitigated in regard to expansion of renewable energy and conservation of marine biodiversity.

The number of megafauna in the sea, feeding, and breeding on or close to the seabed, is innumerable. The sediment erosion potential of these biological agents deserves more attention in the marine research community. Seafloor morphology modulated by vertebrate macro-bioturbation with subsequent scouring may actually represent unique geologic facies that has been misinterpreted as pockmarks before.

## Methods

**Multibeam data acquisition.** Data were acquired during five research cruises using three different multibeam echosounder systems (MBES) in 2013 (HE400<sup>66</sup>), 2017 (HE478<sup>67</sup>), and 2021 (MSM98<sup>68</sup>, HE576, HE588; Supplementary Table 1). The data from R/V Heincke in 2013, 2017, and 2021 were acquired with a KONGSBERG EM710 which was used in combination with a PHINS II (iXsea) motion reference unit. The System operates with  $0.5 \times 1^\circ$  RX/TX transducers and acquires 400 soundings per ping. The FM chirp transmits frequencies between 70–100 kHz. For positioning we used the onboard DGPS providing accuracies

in the decimeter scale. On R/V Merian, we employed the permanently installed KONGSBERG multibeam system EM712 consisting of a  $0.5 \times 0.5^\circ$  RX/TX transducer array coupled to a Seapath inertial navigation unit. We operated the MBES with a frequency modulated chirp between 70–100 kHz. Dual-ping mode, where one swath is slightly tilted forward and the second swath slightly tilted towards the aft of the vessel, was used to increase sounding density. For the highest possible resolution, we installed a modern NORBIT iWBMS shallow water multibeam echosounder system together with an Applanix Wavemaster II inertial navigation unit into the moonpool of R/V Merian<sup>68</sup>. The echosounder was run with 400 kHz in chirp mode with 80 kHz bandwidth resulting in a theoretical range resolution of 0.009 m. Our GNSS measurements were aided using real time kinematics (RTK) supported by a local GNSS reference station and corrections were kindly provided by Axionet GmbH resulting in position and height accuracies ranging between 0.02–0.05 m. Sound velocity was measured online with an AML keel probe as well as with vertical casts.

We calibrated the multibeam data for roll pitch and yaw using Qimera, where we also corrected for water column refraction and tide through integration of backward modeled water level time series (kindly provided by the Federal Hydrographic Agency, BSH). According to sea-state and resulting outliers the soundings were spline filtered using various filter strengths. Especially with the NORBIT 400 kHz data we sailed slow survey lines during good weather leading to very clean point cloud data without the need of manual flagging or filtering. Those data were directly visualized by routines in GMT<sup>69</sup>. The majority of the MBES data was interpolated to a  $1 \times 1$  m grid and visualized in QGIS 3.16.

**Algorithm for automated mapping of seafloor depressions in MBES data.** We mapped the seabed depressions using a combination of geoprocessing tools within the ArcMap software (see also<sup>70</sup>). First, all circular depressions located entirely within a multibeam stripe were filled up to their pour point defining the lowest elevation along their rim. Subsequently, the filled grid was subtracted from the original data resulting in a new grid that defines the difference in height between the original and the filled dataset. Polygons were then drawn automatically around regions that had changed by 0.05 m or more (i.e., a height value of  $\geq 0.05$  m in the differential grid). Holes within individual polygons were filled when their area was smaller than half of the entire polygon. The outline of the polygons was smoothed using a Polynomial Approximation with Exponential Kernel (PEAK) algorithm. Afterwards we calculated the area of the polygons and removed all features with a size below  $10 \text{ m}^2$ . This step was necessary to remove a large number of polygons that did not encircle a seabed depression but rather resulted from noise in the multibeam data. Afterwards a visual inspection of the automatically mapped polygons was conducted and some additional polygons that did not outline a seabed depression were manually removed. For this final dataset of polygons, we then calculated the area, mean, and maximum depth.

**Sidescan sonar.** We used an Edgetech 4200MP dual pulse sidescan sonar system to acquire high-resolution backscatter images of the seafloor. The system emitted a chirp signal with a center frequency of 300 kHz with a vertical beamwidth of  $50^\circ$  on either side and a horizontal beamwidth of  $0.5^\circ$ . The sidescan sonar was towed with a constant cable length, about 10 m above the seafloor at ship speed between 4 and 5 knots. The range of the EdgeTech 4200MP was set to 140 m and 230 m on each side during HE400 and HE478 respectively. All data was stored in.jsf file format and postprocessed using Chesapeake Technology SonarWiz software.

**Parametric sub-bottom profiling.** All surveys were accompanied by sub-bottom profiling to better understand the geological setting and in order to identify shallow gas as one possible driver for pockmark formation. On R/V Merian we employed the parametric PARASOUND System DS3 (P70) manufactured by TEL-EDYNE ATLAS HYDROGRAPHIC GmbH. We selected 19.3 kHz as the fixed Primary Low Frequency (PLF) that distributes energy within a beam of  $\sim 4.5^\circ$ . The system was operated with a maximum transmission voltage of 160 V and achieved a sediment penetration of approx. 13 meters before the multiple reflection of the seafloor interfered with the signal. On R/V Heincke we used an INNOMAR SES-2000 medium. The sub-bottom profiler generated secondary low frequencies between 6 and 15 kHz and data were analyzed using IHS Kingdom software. Motion compensation was achieved using the ship's Photonic Inertial Navigation System motion sensor PHINS II.

**Groundtruthing.** We used an underwater camera system (drop-cam) to obtain video footage of the seafloor. The device consists of 2 forward-looking cameras with a tail fin to passively rotate the system into the prevailing currents. Four artificial light sources and a laser scaler for size reference were used. We towed the system at a constant height of  $\sim 1$  m above the seafloor while occasional drops of the system onto the seafloor allowed us to acquire stationary footage from one spot. R/V Heincke's DGPS system assured an accurate positioning of the system on the seafloor.

We acquired a total of 45 sediment samples using a HELCOM grab sampler on the Sylt Outer Reef to verify the acoustic backscatter response of the seafloor. The samples were scraped off from the upper 2 cm of the sediment surface in a HELCOM Van Veen grab sampler. We removed shell fragments (carbonates) and organic matter from the samples using acetic acid and hydrogen peroxide. The grain size distribution of each sample was subsequently analyzed using a CILAS 1180 laser-diffraction particle analyzer after sieving off gravel parts if present. The instrument measures at a bandwidth of 14.6–1.4  $\Phi$  (0.04–2500  $\mu\text{m}$ ), which was sufficient for the samples taken. Grain size statistics were subsequently calculated using the software package 'Gradistat' after.

**Harbor porpoise density modeling.** To estimate abundance of harbor porpoises in the area of investigation, we extracted numbers from published seasonal habitat-based density models covering the southern North Sea<sup>56</sup>. This enabled to calculate the total abundance of harbor porpoise in our study area. The prediction of harbor porpoise density is based on generalized additive models fitted to visual airborne survey data, collected in 2005–2013 by dedicated line-transect sampling, using predictor variables such as water depth, distance to shore and to sandeel (*Ammodytes spp.*) grounds, sea surface temperature, proxies for fronts, and day length<sup>56</sup>.

#### Data availability

The hydroacoustic, video, and grab sample data from HE400 and HE478 are available for public download ([www.pangaea.de](http://www.pangaea.de), <https://doi.org/10.1594/PANGAEA.899501>). The subsequently recorded ship-born data have all been uploaded to the repository of the German Federal Hydrographic Agency (BSH), and still have a moratorium expiring in 2023, and will then be available on Pangaea. All cruises meta information are accessible via the [www.pangaea.de](http://www.pangaea.de) portal.

Received: 2 February 2023; Accepted: 13 November 2023;

Published online: 19 December 2023

#### References

- Judd, A. & Hovland, M. *Seabed Fluid Flow: The Impact on Geology, Biology and the Marine Environment* (Cambridge Univ. Press, 2009).
- King, L. H. & MacLEAN, B. Pockmarks on the Scotian shelf. *Geol. Soc. Am. Bull.* **81**, 3141–3148 (1970).
- Whiticar, M. J. & Werner, F. Pockmarks: submarine vents of natural gas or freshwater seeps? *Geo-Mar. Lett.* **1**, 193–199 (1981).
- Pickrill, R. A. Shallow seismic stratigraphy and pockmarks of a hydrothermally influenced lake, Lake Rotoiti, New Zealand. *Sedimentology* **40**, 813–828 (1993).
- Kelley, J. T., Dickson, S. M., Belknap, D. F., Barnhardt, W. A. & Henderson, M. Giant sea-bed pockmarks: evidence for gas escape from Belfast Bay, Maine. *Geology* **22**, 59–62 (1994).
- Hoffmann, J. J. L. et al. Complex eyed pockmarks and submarine groundwater discharge revealed by acoustic data and sediment cores in Eckernförde Bay, SW Baltic Sea. *Geochem. Geophys. Geosyst.* **21**, e2019GC008825 (2020).
- Pilcher, R. & Argent, J. Mega-pockmarks and linear pockmark trains on the West African continental margin. *Mar. Geol.* **244**, 15–32 (2007).
- Harris, P. & Baker, E. *Seafloor Geomorphology as Benthic Habitat: GeoHab Atlas of Seafloor Geomorphic Features and Benthic Habitats* (Elsevier, 2011).
- Micallef, A., Krastel, S. & Savini, A. Submarine geomorphology. *Geol. Soc. Lond. Mem.* **58**, 379–394 (2022).
- Schneider von Deimling, J. et al. Quantification of seep-related methane gas emissions at Tommeliten, North Sea. *Cont. Shelf Res.* **31**, 867–878 (2011).
- Micallef, A. et al. Multiple drivers and controls of pockmark formation across the Canterbury Margin, New Zealand. *Basin Res.* **34**, 1374–1399 (2022).
- Klaucke, I. et al. Giant depressions on the Chatham Rise offshore New Zealand—morphology, structure and possible relation to fluid expulsion and bottom currents. *Mar. Geol.* **399**, 158–169 (2018).
- Paull, C. et al. Pockmarks off Big Sur, California. *Mar. Geol.* **181**, 323–335 (2002).
- Iglesias, J., Ercilla, G., Garcia-Gil, S. & Judd, A. G. Pockforms: an evaluation of pockmark-like seabed features on the Landes Plateau, Bay of Biscay. *Geo-Mar. Lett.* **30**, 207–219 (2010).
- Hoffmann, J. J., Michaelis, R., Mielck, F., Bartholomä, A. & Sander, L. Multiannual seafloor dynamics around a subtidal rocky reef habitat in the North Sea. *Remote Sens.* **14**, 2069 (2022).
- Macdonald, H. A. et al. New insights into the morphology, fill, and remarkable longevity (>0.2 m.y.) of modern deep-water erosional scours along the northeast Atlantic margin. *Geosphere* **7**, 845–867 (2011).
- Johnson, K. R. & Nelson, C. H. Side-scan sonar assessment of gray whale feeding in the Bering Sea. *Science* **225**, 1150–1152 (1984).
- Nelson, C. H., Johnson, K. R. & Barber, J. H. Gray whale and walrus feeding excavation on the Bering Shelf, Alaska. *J. Sediment. Res.* **57**, 419–430 (1987).
- Mueller, R. J. Evidence for the biotic origin of seabed pockmarks on the Australian continental shelf. *Mar. Pet. Geol.* **64**, 276–293 (2015).
- Mueller, R. Response to comments by Nicholas et al. (2016) on 'Evidence for the biotic origin of seabed pockmarks on the Australian continental shelf'. *Mar. Pet. Geol.* **69**, 262–265 (2016).
- Nicholas, W. A., Nichol, S. L., Kool, J., Carroll, A. & Rollet, N. Comment on "Evidence for the biotic origin of seabed pockmarks on the Australian continental shelf" by R.J. Mueller [Marine and Petroleum Geology (2015)]. *Mar. Pet. Geol.* **69**, 266–268 (2016).
- Purser, A. et al. A vast icefish breeding colony discovered in the Antarctic. *Curr. Biol.* **32**, 842–850.e4 (2022).
- Judd, A. et al. Contributions to atmospheric methane by natural seepages on the UK continental shelf. *Mar. Geol.* **137**, 165–189 (1997).
- Judd, A. G. *A review of pockmarks in the UK part of the North Sea, with particular respect to their biology*. Technical Report No. 22 (School of Ocean Sciences, University of Wales-Bangor, 2001).
- Krämer, K. et al. Abrupt emergence of a large pockmark field in the German Bight, southeastern North Sea. *Sci. Rep.* **7**, 1–8 (2017).
- Coughlan, M. et al. A revised stratigraphical framework for the Quaternary deposits of the German North Sea sector: a geological-geotechnical approach. *Boreas* **47**, 80–105 (2018).
- Ahrendt, K. & Tabat, W. Ein Vierteljahrhundert sedimentologische Forschung vor der Küste Sylts/Deutsche Bucht. *Meyniana* **46**, 11–36 (1994).
- Bockelmann, F.-D., Puls, W., Kleeberg, U., Mueller, D. & Emeis, K.-C. Mapping mud content and median grain-size of North Sea sediments – a geostatistical approach. *Mar. Geol.* **397**, 60–71 (2018).
- Diesing, M., Kubicki, A., Winter, C. & Schwarzer, K. Decadal scale stability of sorted bedforms, German Bight, southeastern North Sea. *Cont. Shelf Res.* **26**, 902–916 (2006).
- Feldens, P., Schulze, I., Papenmeier, S., Schönte, M. & Schneider von Deimling, J. Improved interpretation of marine sedimentary environments using multi-frequency multibeam backscatter data. *Geosciences* **8**, 214 (2018).



31. Bartholomä, A., Capperucci, R. M., Becker, L., Coers, S. I. I. & Battershill, C. N. Hydrodynamics and hydroacoustic mapping of a benthic seafloor in a coarse grain habitat of the German Bight. *Geo-Mar. Lett.* **40**, 183–195 (2020).
32. Belkin, I. M., Cornillon, P. C. & Sherman, K. Fronts in large marine ecosystems. *Prog. Oceanogr.* **81**, 223–236 (2009).
33. Römer, M. et al. Seafloor methane seepage related to salt diapirism in the northwestern part of the German North Sea. *Front. Earth Sci.* **9**, 556329 (2021).
34. Karstens, J. et al. Formation of the Figge maar seafloor crater during the 1964 B1 blowout in the German North Sea. *Earth Sci. Syst. Soc.* **2**, 10053 (2022).
35. de Haas, H., Boer, W. & van Weering, T. C. E. Recent sedimentation and organic carbon burial in a shelf sea: the North Sea. *Mar. Geol.* **144**, 131–146 (1997).
36. Lohrberg, A. et al. Discovery and quantification of a widespread methane ebullition event in a coastal inlet (Baltic Sea) using a novel sonar strategy. *Sci. Rep.* **10**, 1–13 (2020).
37. Papenmeier, S. & Hass, H. C. Revisiting the paleo Elbe Valley: reconstruction of the Holocene, sedimentary development on basis of high-resolution grain size data and shallow seismics. *Geosciences* **10**, 505 (2020).
38. Rehder, G., Keir, R. S., Suess, E. & Pohlmann, T. The multiple sources and patterns of methane in North Sea waters. *Aquat. Geochem.* **4**, 403–427 (1998).
39. Schneider von Deimling, J., Linke, P., Schmidt, M. & Rehder, G. Ongoing methane discharge at well site 22/4b (North Sea) and discovery of a spiral vortex bubble plume motion. *Mar. Pet. Geol.* **68**, 718–730 (2015).
40. Nachtsheim, D. A. et al. Small cetacean in a human high-use area: trends in harbor porpoise abundance in the North Sea over two decades. *Front. Mar. Sci.* **7**, 606609 (2021).
41. Johnston, C. & Berta, A. Comparative anatomy and evolutionary history of suction feeding in cetaceans. *Mar. Mammal Sci.* **27**, 493–513 (2011).
42. Leopold, M. F. *Eat and Be Eaten: Porpoise Diet Studies*. PhD dissertation, Wageningen Univ. Res. (2015).
43. Otani, S. et al. Diving behavior and performance of harbor porpoises, *Phocoena phocoena*, in Funka Bay, Hokkaido, Japan. *Mar. Mammal Sci.* **14**, 209–220 (1998).
44. Gilles, A., Andreasen, H., Müller, S. & Siebert, U. Nahrungsökologie von marinen Säugetieren und Seevögeln für das Management von NATURA 2000 Gebieten. *Teil Mar. Säugetiere Final Rep. Submitt. Ger. Fed. Agency Nat. Conserv. BfN F E FKZ* **805**, 018 (2008).
45. Lockyer, C. *EPIC - Elimination of Harbour Porpoise Incidental Catches: Final report for the period 1 June 1998-31 July 2000*. <https://orbit.dtu.dk/en/publications/epic-elimination-of-harbour-porpoise-incident-catches-final-rep> (2000).
46. Desportes, G., Amundin, M. & Goodson, D. Investigate porpoise foraging behaviour-Task1. *Tail EPIC-Elimin. Harb. Porpoise Incidental Catch Final Rep. Eur. Comm. Proj. No DG* **14**, 00006 (2000).
47. Clausen, K. T., Wahlberg, M., Beedholm, K., Deruiter, S. & Madsen, P. T. Click communication in harbour porpoises *Phocoena phocoena*. *Bioacoustics* **20**, 1–28 (2011).
48. Obst, B. S. & Hunt, G. L. Marine birds feed at gray whale mud plumes in the Bering Sea. *The Auk* **107**, 678–688 (1990).
49. Marsh, L., Huvenne, V. A. & Jones, D. O. Geomorphological evidence of large vertebrates interacting with the seafloor at abyssal depths in a region designated for deep-sea mining. *R. Soc. Open Sci.* **5**, 180286 (2018).
50. Purser, A. et al. Depression chains in seafloor of contrasting morphology, Atacama Trench margin: a comment on Marsh et al. (2018). *R. Soc. Open Sci.* **6**, 182053 (2019).
51. Rossbach, K. A. & Herzing, D. L. Underwater Observations of Benthic-Feeding Bottlenose Dolphins (*Tursiops Truncatus*) Near Grand Bahama Island, Bahamas. *Mar. Mammal Sci.* **13**, 498–504 (1997).
52. Engleby, L. K. & Powell, J. R. Detailed observations and mechanisms of mud feeding by common bottlenose dolphins (*Tursiops truncatus truncatus*) in Florida Bay, Florida, U.S.A. *Mar. Mammal Sci.* **35**, 1162–1172 (2019).
53. Simpson, J. H. & Sharples, J. *Introduction to the Physical and Biological Oceanography of Shelf Seas* (Cambridge Univ. Press, 2012).
54. McGlade, J. M. 12 The North Sea Large Marine Ecosystem. In *Large Marine Ecosystems*, (Eds Sherman, K. & Skjoldal, H. R.) Vol. 10 339–412 (Elsevier, 2002).
55. Holt, J. & Umlauf, L. Modelling the tidal mixing fronts and seasonal stratification of the Northwest European Continental shelf. *Cont. Shelf Res.* **28**, 887–903 (2008).
56. Gilles, A. et al. Seasonal habitat-based density models for a marine top predator, the harbor porpoise, in a dynamic environment. *Ecosphere* **7**, e01367 (2016).
57. Benjamins, S., Dale, A., van Geel, N. & Wilson, B. Riding the tide: use of a moving tidal-stream habitat by harbour porpoises. *Mar. Ecol. Prog. Ser.* **549**, 275–288 (2016).
58. Jensen, H., Rindorf, A., Wright, P. J. & Mosegaard, H. Inferring the location and scale of mixing between habitat areas of lesser sandeel through information from the fishery. *ICES J. Mar. Sci.* **68**, 43–51 (2011).
59. van Deurs, M., Hartvig, M. & Steffensen, J. F. Critical threshold size for overwintering sandeels (*Ammodytes marinus*). *Mar. Biol.* **158**, 2755–2764 (2011).
60. Greene, H. G., Baker, M. & Aschoff, J. A dynamic bedforms habitat for the forage fish Pacific sand lance, San Juan Islands, WA, United States. In *Seafloor Geomorphology as Benthic Habitat* (Eds Harris, P. T. & Baker, E.) 267–279 (Elsevier, 2020).
61. Wisniewska, D. M. et al. Ultra-high foraging rates of harbor porpoises make them vulnerable to anthropogenic disturbance. *Curr. Biol.* **26**, 1441–1446 (2016).
62. Hillman, J. I. et al. The influence of submarine currents associated with the Subtropical Front upon seafloor depression morphologies on the eastern passive margin of South Island, New Zealand. *N. Z. J. Geol. Geophys.* **61**, 112–125 (2018).
63. Dick, S. Gezeitenströmungen um Sylt Numerische Untersuchungen zur halbtägigen Hauptmond tide (M 2). *Dtsch. Hydrogr. Z.* **40**, 25–44 (1987).
64. Ferrini, V. L. & Flood, R. D. A comparison of rippled scour depressions identified with multibeam sonar: evidence of sediment transport in inner shelf environments. *Cont. Shelf Res.* **25**, 1979–1995 (2005).
65. Davis, A. C. et al. Distribution and abundance of rippled scour depressions along the California coast. *Cont. Shelf Res.* **69**, 88–100 (2013).
66. Hass, H. C. & Papenmeier, S. Swath sonar bathymetry during R/V Heincke cruise HE400 with links to multibeam raw data files <https://doi.org/10.1594/PANGAEA.899501> (Alfred Wegener Institute - Wadden Sea Station Sylt, 2019).
67. Papenmeier, S. & Hass, H. C. Swath sonar bathymetry during R/V Heincke cruise HE478 with links to multibeam raw data files <https://doi.org/10.1594/PANGAEA.899835> (Alfred Wegener Institute - Wadden Sea Station Sylt, 2019).
68. Schneider von Deimling, J. RV MARIA S. MERIAN MSM98/2 Cruise Report No. 56 [https://doi.org/10.48433/cr\\_msm98\\_2](https://doi.org/10.48433/cr_msm98_2) (2022).
69. Wessel, P. & Smith, W. H. New, improved version of Generic Mapping Tools released. *Eos Trans. Am. Geophys. Union* **79**, 579–579 (1998).
70. Böttner, C. et al. Pockmarks in the Witch Ground Basin, Central North Sea. *Geochem. Geophys. Geosyst.* **20**, 1698–1719 (2019).

## Acknowledgements

We acknowledge the support from the German Research Fleet Coordination Centre with organization and support for marine research and cruises under the COVID19 pandemic. We appreciate the support of the German Research Foundation (DFG) that enabled the RV Merian cruise MSM98/2 (Grant no GPF20-3\_073), during which the hypothesis was developed. The cruises HE400 and HE478 were part of SedAWZ and received support from the German Federal Maritime and Hydrographic Agency (BSH) and the German Federal Agency for Nature Conservation (BfN). Our memories are with H.C. Hass who was one of the project founders and the cruise leader of HE400. Funding for HE576 and HE588 was received through the BMBF-funded 'DAM pilot mission: Exclusion of mobile bottom-contact fishing in marine protected areas of the German EEZ of the North Sea and Baltic Sea' [Grant no. 03F0847A]. This research was additionally supported by the Marie Curie action KARST, under the EU H2020 program, project number 101027303. Recent data on diet of harbor porpoises were collected by E. Hesse in BioWeb [Grant no. 03F0861D] funded by the German Federal Ministry of Education and Research (BMBF) within the framework program "Research for sustainable development - FONAS3". We also appreciate valuable discussions with the oceanmindfoundation.org about whale behavior during our field survey and discovery of the pits. The authors express their sincere thanks to the captains and crews of R/V Heincke and R/V Merian who enabled the measurements even in winter times under severe weather conditions in the North Sea.

## Author contributions

J.S.v.D. developed the hypothesis, designed the research study, and led the writing of the manuscript together with J.G. and J.H. J.H., S.P., A.L., and J.S.v.D. acquired the data. J.H. and J.S.v.D. processed the multibeam data. J.S.v.D. designed all figures and detected the SST tidal mixing front together with I.B., who also reviewed the oceanographic setting. J.G. developed and implemented statistical analyses. J.S.v.D., J.G., J.H., S.Ko., and S.K. mainly wrote the manuscript. S.Ko. contributed early to the discussion of the hypothesis with expert knowledge on harbor porpoise behavior and physiology. A.G. supported the calculations based on harbor porpoise abundance models as well as diet studies. C.B., A.L., and S.P. supported the discussion with their expert knowledge in the North Sea. All authors contributed to the overall interpretation of the data and final evaluation.

## Funding

Open Access funding enabled and organized by Projekt DEAL.

## Competing interests

The authors declare no competing interests.

**Additional information**

**Supplementary information** The online version contains supplementary material available at <https://doi.org/10.1038/s43247-023-01102-y>.

**Correspondence** and requests for materials should be addressed to Jens Schneider von Deimling.

**Peer review information** *Communications Earth & Environment* thanks Alan Judd, Deniz Cukur, and the other, anonymous, reviewer(s) for their contribution to the peer review of this work. Primary Handling Editors: Andrew Green and Joe Aslin. A peer review file is available

**Reprints and permission information** is available at <http://www.nature.com/reprints>

**Publisher's note** Springer Nature remains neutral with regard to jurisdictional claims in published maps and institutional affiliations.



**Open Access** This article is licensed under a Creative Commons Attribution 4.0 International License, which permits use, sharing, adaptation, distribution and reproduction in any medium or format, as long as you give appropriate credit to the original author(s) and the source, provide a link to the Creative Commons licence, and indicate if changes were made. The images or other third party material in this article are included in the article's Creative Commons licence, unless indicated otherwise in a credit line to the material. If material is not included in the article's Creative Commons licence and your intended use is not permitted by statutory regulation or exceeds the permitted use, you will need to obtain permission directly from the copyright holder. To view a copy of this licence, visit <http://creativecommons.org/licenses/by/4.0/>.

© The Author(s) 2023